An operational calculus framework to characterize droplet size populations from turbulent breakup by a small number of parameters

2010 J. Phys. A: Math. Theor. 43 185501

(http://iopscience.iop.org/1751-8121/43/18/185501)

IOP PUBLISHING JOURNAL OF PHYSICS A: MATHEMATICAL AND THEORETICAL

J. Phys. A: Math. Theor. **43** (2010) 185501 (22pp) doi:10.1088/1751-8113/43/18/185501

An operational calculus framework to characterize droplet size populations from turbulent breakup by a small number of parameters

Rafael Vázquez and Alfonso M Gañán-Calvo

Departamento de Ingeniería Aeroespacial y Mecánica de Fluidos, Universidad de Sevilla, e-41092 Sevilla, Spain

E-mail: amgc@us.es

Received 20 October 2009, in final form 17 March 2010
Published 15 April 2010
Online at stacks.iop.org/JPhysA/43/185501

Abstract

A systematic operational calculus framework that characterizes droplet/bubble size distributions resulting from turbulent breakup of an immiscible fluid into a carrier one is presented. The proposed formulation is derived from dynamical arguments; a finite-difference formulation of the integro-differential continuous coagulation and fragmentation equation is shown to exhibit the same structure as a discrete sequence of Mellin convolutions between the probability distribution of the evolving dispersed phase and a generic kernel. This kernel may have its physical correspondence with the probability distribution resulting from a single breakup event, e.g. a liquid ligament breakup in a ligament-mediated spray formation. The number of convolution steps in the sequence can be reduced to a single parameter. As an illustration, this procedure is applied to the exponential and the gamma distributions, obtaining as a result the Fréchet distribution earlier used by Rosin and Rammler (1934 *Kolloid-Zeitschrift* **67** 16–26), and by Nukiyama and Tanasawa (1939 *Trans. Soc. Mech. Eng. Japan* **5** 62–7). Thus, the framework introduced in this work provides a physical foundation for the success of the Fréchet distribution in accurately fitting experimentally measured droplet size distributions in sprays and emulsions.

PACS numbers: 47.55.D−, 02.50.Cw

(Some figures in this article are in colour only in the electronic version)

1. Introduction

Complex physical processes involving a multiplicity or even a continuum of scales frequently induce the emergence of large-scale features and behaviors amenable to description in terms of

a finite number of parameters, an understanding whose accomplishment is foreseen by some authors of prospective essays as one of the various fundamental opportunities of physics in this century [1]. Among complex processes, turbulent breakup and dispersion of an immiscible phase into a carrier one may well be one of the most paradigmatic cases for its ubiquity, prevalence and overall importance in many natural and artificial activities.

Since the early works of Kolmogorov [2] and Hinze [3], the understanding and quantification of the processes taking place on the turbulent breakup and dispersion of immiscible phases have undergone a significant advance [4]. The physical and chemical characteristics of the final dispersion are determined by a great extent by the size distribution of the droplet or bubble populations. The energy transfer from the carrier to the dispersed phase in the form of droplets or bubbles involves complex processes where interfacial, viscous and inertia forces play different roles depending on the local characteristic lengths considered [5].

Generically, the amount of energy that the process manages to put in the form of interfacial free energy can be quantified by a single parameter, the well-known Sauter mean diameter, which measures the inverse of the amount of surface produced per unit volume dispersed in the process. However, a single parameter cannot provide any additional fundamental information on the eventually resulting state, such as the extension of the small and large size tails of the distribution, the amount of mass contained in the population below a given size, the possible existence of multiple peaks in the count or mass distribution or the general appearance of the size population. These features are best described considering the population size as a random variable and analyzing its probability distribution, mathematically expressed as a continuous function. The methods of mathematical statistics allow us to study the asymptotic behavior of a dynamical process acting on a random variable; for instance, one of the most important results in statistics, the central limit theorem, reduces to a universal function class, the normal (or its alternative log-normal distribution), the asymptotic distribution of an infinite sum (or product) of random variables under rather general hypotheses. In the case of turbulent breakup, an 'asymptotic' distribution would involve a large number of steps or a long processing time, under constant energy input and geometrical scales. However, most real processes like the pneumatic atomization of a liquid are characterized by a short time of development (the residence time of the liquid at the nozzle discharge region). Thus, the resulting spray statistics should reflect the fact that the process (i) underwent strongly varying conditions under enormous gradients and (ii) became halted soon before asymptotic conditions could be even approached.

The quest for the links between the statistical properties of the resulting size distribution and the dynamical events taking place during the finite-time turbulent breakup, mixing and dispersion process has traditionally been one of the fundamental topics of multiphase flow physics. Both fragmentation and coalescence events plague the intimate contact between the carrier and the disperse phase in their co-evolution, to such an extent that these could be considered the basic ingredients of every turbulent breakup and dispersion process, being the carrier phase the main source of energy. Numerous studies on the mathematical features of the solutions to either coalescence of fragmentation equations (i.e. existence and uniqueness, similarity, asymptotic behaviors, etc) have been proposed (e.g. [6–10]). In this regard, numerous authors have resorted to either fragmentation (e.g. [11–14]) or coalescence phenomena alone [15, 16] to explain the basic features of different distributions resulting from breakup phenomena. In these last references, Villermaux, Marmottant and collaborators claimed to explain the resulting general size distribution of droplets in sprays in terms of liquid coalescence events during liquid ligament breakup, leading to gamma distributions. Indeed, they successfully compare with experiments their proposition in detailed studies on liquid ligament breakup (see also [17]). It is interesting to emphasize that their ideas are

not explained from fragmentation but from coalescence principles alone. Moreover, in the preparation of the present paper, an article by Villermaux and Bosa [18] has appeared analyzing in detail the dynamics of formation of rain droplets. These authors describe the rain droplet size distribution from the convolution of a gamma distribution previously proposed by them (due to the breakup of liquid rims resulting from bag-like breakup of droplets larger than a critical size) and an exponential distribution (from the large size tail of prior ligament breakups) to obtain a size distribution law that seems to explain prior findings. Intriguingly, these authors do not explain the raindrop size distribution from fragmentation principles, what might seem obvious at first sight: the ultimate mechanism that describes their specific proposed distribution is *coalescence*, instead. Fragmentation is just a random route to reach the specific critical size that gives rise to a single-bag breakup mode (which seems the ultimate breakup mechanism of rain droplets); the droplets around the critical size have an exponential distribution in that range because they come from the large size tail of prior breakups following gamma distributions.

Some authors have already pointed out the analogy between the equations of coalescence and fragmentation (e.g. [9, 19, 20]), and consequently it seems natural to propose combined forms of these equations applicable to processes where both phenomena may coexist [10]. These expressions may provide a natural, useful tool to mathematically describe the turbulent breakup of immiscible phases. Thus, motivated by the structure of the non-linear integro-differential equation modeling coagulation and fragmentation already proposed in the literature [10], in this work we propose a mathematical framework (based on the Mellin transform) to study the resulting size distribution. Using our formulation, we generalize a variety of previously proposed distributions. These generalized distributions exhibit universal features with direct physical interpretation. In particular, we lay out a generalization of previous approaches [15] where only coalescence or fragmentation [14] events were considered. As already pointed out through the step taken in [18], those previous approaches may provide basic but incomplete ingredients to find the droplet size distribution of a generic real spray.

In summary, our aim is to introduce a mathematical framework where real droplet distributions resulting from turbulent breakup processes could be faithfully *projected* on simple functional spaces provided by continuous mathematical functions (continuous probability distributions). These functions are characterized by a small number of meaningful parameters which encapsulate physical features of the process, such as characteristic lengths, frequencies or average number of coalescence/fragmentation events. In this work, we apply our proposed approach to analyze two families of classical, well-established model probability density functions (pdfs), showing the deep physical roots of their enormous success to describe real distributions by explaining the physical meaning of their free parameters. We show that a physically consistent, general mathematical reduction along the lines here proposed may successfully complement, generalize or expand the applicability of prior studies like the ones by [15, 16], in the context of the spray formation from liquid ligament turbulent breakup, and by other authors (e.g. [19, 21]) who studied the asymptotic solutions to the fragmentation equations.

2. Mathematical structure of mass-conservative probability density functions, and proposed general approaches

In general, a pdf used to describe the random distribution of lengths, surfaces or volumes and, in particular, the distribution of the mass or volumes of droplets or bubbles in a spray,

emulsion or foam can be written in the form

$$p(x) = x^{\alpha-1} f(x), \tag{1}$$

where x represents the droplet mass or volume. Clearly, $f(x)$ must obey obvious conditions of integrability in the domain $x \in [0, \infty)$, demanded by mass conservation and existence of all moments of the distribution $p(x)$. Here, in contrast with other studies [15, 16], we use the droplet or bubble mass as the relevant variable for its generality and independence from the particular geometry of the particle, and for convenience to express simple mass conservation principles as follows.

2.1. Count median and mass median size

The *mass mean* size is taken as the unity of mass in this work, i.e.

$$\int_0^\infty x p(x,t)\,\mathrm{d}x = 1. \tag{2}$$

Using the definition of the Mellin transform $P(s)$ of $p(x)$ (appendix A), equation (2) implies that

$$P(2) = 1. \tag{3}$$

Similarly one has that $P(1) = 1$ because $p(x)$ is a probability density function.

We define the *count median* particle mass x_{50} as

$$\int_0^{x_{50}} p(x,t)\,\mathrm{d}x = 1/2, \tag{4}$$

and the particle *mass median* size y_{50} as

$$\int_0^{y_{50}} x p(x,t)\,\mathrm{d}x = 1/2. \tag{5}$$

If we were interested in the mass fraction ϕ of the total mass put in mass sizes smaller than y_ϕ, it would be calculated through the expression

$$\phi = \int_0^{y_\phi} x p(x,t)\,\mathrm{d}x. \tag{6}$$

2.2. A finite-difference reduction of the general fragmentation–coagulation equations

The complexity and case-dependency exhibited by the exhaustive studies already existing in the literature preclude the general treatment pursued in this work. On the other hand, a sufficiently general approach should be consistent with the basic, common dynamical ingredients shared by all turbulent breakup phenomena, i.e. it must encompass fragmentation, collision and coalescence and dynamical evolution in a mathematical formulation as general and consistent as possible. Ideally, we seek for a reduction of the dynamical effects mentioned into a finite number of parameters. To deal with this challenge, the choice of the structure (1) is not arbitrary. While the multiplicative factor $x^{\alpha-1}$ reflects the general trend of the distribution for small sizes (sometimes due to fragmentation), $f(x)$ is often given in the form of exponential expressions; interestingly, the log-normal, exponential, Poisson or gamma, Fréchet (also known as Rosin-Rammler, Nukiyama-Tanasawa, or Weibull [22–25]), and other proposed distributions follow this simple structure. A physical foundation for the exponential nature of $f(x)$ is proposed in [15], where the authors explain the exponential decay e^{-x} of drop sizes as a result of the ligament-mediated spray formation on the basis of coalescence events of the randomly distributed liquid lumps in which a ligament is composed of.

To formulate a mathematical model for $f(x)$ as simple as possible, we make use of a recently proposed general formulation of the dynamical fragmentation–coagulation equation [10]. Our partial goal is here to characterize the general effect that a cascade of several subsequent fragmentation–coagulation events would leave onto an initial pdf, ideally reflected by a *single* parameter. We model those events as dynamical 'convolutions' of the pdf and a generic kernel; thus, the parameter will allow us to determine the degree of convolution that a certain process imposes. Since each convolution represents a product of random variables, the consistency of the proposed mathematical transformations is tested against the central limit theorem when the degree of convolution becomes large: our proposed transformations should convert any initial pdf into a log-normal as the degree of convolution grows.

Fragmentation–coagulation equations, both in discrete [26] and continuous [10] forms, have been formulated in the literature, and the existence and uniqueness of their solutions have been studied in some depth. Moreover, asymptotic/equilibrium solutions have also been given. The general form of continuous fragmentation–coagulation equations can be written as [10]

$$\partial_t p(x,t) = (\mathcal{F}p)(x,t) + (\mathcal{C}p)(x,t), \tag{7}$$

where $p(x, t)$ represents the probability density function of a lump of liquid of mass x at time t. $\mathcal{F}$ and $\mathcal{C}$ are the operators representing the production rates per unit time from fragmentation and coalescence, respectively. They are more explicitly written in the literature as

$$(\mathcal{F}p)(x,t) = -a(x)p(x,t) + \int_x^\infty b(x,y)a(y)p(y,t)\,\mathrm{d}y, \tag{8}$$

and

$$\begin{aligned}(\mathcal{C}p)(x,t) = &\int_0^x \frac{1}{2}k(x-y,y)p(x-y,t)p(y,t)\,\mathrm{d}y \\ &- p(x,t)\int_0^\infty k(x,y)p(y,t)\,\mathrm{d}y,\end{aligned} \tag{9}$$

where a more detailed explanation of each term in (8) and (9) is given in [10, 19, 20, 27]. In particular, $a(x)$ represents the overall fragmentation *frequency* of a mass x, $b(x, y)$ represents the average number of lumps of mass x produced when a lump of mass y breaks, which should satisfy $\int_0^y b(x,y)x\,\mathrm{d}x/y = 1$ for conservation of mass and $k(x, y)$ represents the coalescence frequency of masses with sizes x and y.

We will attempt to use the integro-differential equation (7) to represent a *finite* time process (the liquid atomization) which proceeds along a number N of time *steps* Δt before it is abruptly stopped at the final state. To do so, we make a number of broad assumptions on the evolution equation (7), described next, to reach to a very simplified model. How accurately this model may reflect general physical features of actual mass distributions can be quantified afterward through the appropriate experimental comparison with real droplet size distributions.

Given the general form of the *destruction* and *production* terms in (8) and (9), it is possible to make the following observations.

(i) A unified *destructive* term can be written as

$$\begin{aligned}(\mathcal{D}p)(x,t) &= -p(x,t)\int_0^\infty [a(x)+k(x,y)]p(y,t)\,\mathrm{d}y \\ &= -p(x,t)d(x,t),\end{aligned} \tag{10}$$

given that $\int_0^\infty p(y,t)\,\mathrm{d}y = 1$, where $d(x, t)$ can be interpreted as the average, total destruction frequency of a mass x along the process.

(ii) A unified *productive* term is expressible as

$$(\mathcal{P}p)(x,t) = \int_0^\infty \left\{ b(x,y)a(y)H(x) + \frac{1}{2}k(x-y,y)p(x-y,t)\,[1-H(x)] \right\} p(y,t)\,\mathrm{d}y, \tag{11}$$

where $H(x)$ is the Heaviside step function, introduced for consistency with expressions (8) and (9).

(iii) One can approximate the kernel in the integral transform of (11) as

$$p^*(x/y,t)d(y,t)/y \simeq b(x,y)a(y)H(x) + \tfrac{1}{2}k(x-y,y)p(x-y,t)[1-H(x)], \tag{12}$$

where $p^*(x,t)$ is, through mass conservation considerations, a certain probability distribution which might get its physical meaning from the repeated and homogeneously distributed sub-processes of breakup driven by the turbulent frequency and the availability of turbulent energy along the entire x-size scale cascade. Then $(\mathcal{P}p)(x,t)$ could be expressed as

$$(\mathcal{P}p)(x,t) = \int_0^\infty p^*(x/y,t)p(y,t)d(y,t)\,\mathrm{d}y/y. \tag{13}$$

(iv) Using the function $p^*(x,t)$ from (12), one could reduce (7) to a finite difference expression for a time interval Δt as

$$p(x,t+\Delta t) - p(x,t) \simeq \left[-p(x,t)d(x,t) + \int_0^\infty p^*(x/y,t)p(y,t)d(y,t)\,\mathrm{d}y/y \right]\Delta t + O(\Delta t^2). \tag{14}$$

(v) First, assuming that fragmentation is fundamentally driven by the turbulent energy coming from the gas flow, one may expect that the mass median size scales as a critical length l^* such that the surface tension forces σ/l^* and the pressure fluctuations $\rho_g u'^2 \sim \rho_g U_g^2 (l^*/L)^{2/3} \sim \rho_g(\varepsilon l^*)^{2/3}$ balance. ρ_g, U_g, L and ε are the density, macroscopic velocity, length scale and energy dissipation rate of the gas flow, respectively; u' is the characteristic fluctuation velocity at the length scale l. However, this is not the object of this paper since this has already been widely studied and verified in the literature. We are interested in how the droplet size is distributed around the mass median size, commensurate with l^*. To this end, one may observe that the breakup frequency should go to zero for droplets with characteristic lengths l smaller than the critical size range l^*, while for larger droplets, the frequency should scale as $f \sim (\varepsilon/l^2)^{1/3}$, which decreases as $l^{-2/3}$ when l increases. Thus, since $\mathrm{d}f/\mathrm{d}l > 0$ ($\mathrm{d}f/\mathrm{d}l < 0$) for l larger (smaller) than l^*, the maximum breakup frequency should occur around $f^* \sim U_g/(L\,l^2)^{1/3} \sim \rho_g^{2/5}\sigma^{-2/5}U_g^{9/5}L^{-3/5} \sim \rho^{2/5}\sigma^{-2/5}\varepsilon^{3/5}$ for an average size around $l^* \sim \rho_g^{-3/5}\sigma^{3/5}U_g^{-6/5}L^{2/5} \sim \rho^{-3/5}\sigma^{3/5}\varepsilon^{-2/5}$ (thus, $f^* \sim \varepsilon^{1/3}(l^*)^{-2/3}$), and these frequency and length scales dominate both fragmentation and coalescence since they govern the gas motion, which carries the liquid lumps. Consequently, the breakup and coalescence frequency should exhibit a maximum around f^*, which fundamentally affects a characteristic length scale range around l^*. Many authors have proposed models in the classical literature for the specific drop breakage rate in turbulent flows. Ross and Curl [28], and Coulaloglou and Tavlarides [29] proposed a model as

$$f/f^* = c_1(l^*/l)^{2/3}e^{(-l^*/l)^{5/3}}, \tag{15}$$

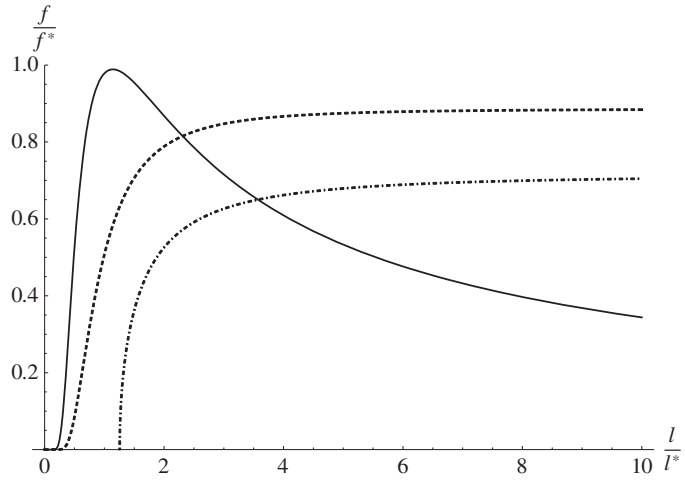

Figure 1. The droplet or bubble breakage rate models of Ross and Curl [28] and Coulaloglou and Tavlarides [29] ($c_1 = 1.6$, $c_2 = 0.5$, continuous line), Chatzi and Lee [31] ($c_1 = 1$, dashed line), and Lasheras *et al* [30] ($c_1 = 0.25$, dot-dashed line).

where $f^* = \varepsilon^{1/3}(l^*)^{-2/3}$, $l^* = \rho^{-3/5}\sigma^{3/5}\varepsilon^{-2/5}$, and $\{c_1, c_2\}$ are the constants of the order unity. This model contains both the $f \sim l^{-2/3}$ trend for l larger than l^* and the decreasing f behavior for l smaller than l^*. The model above was reviewed by Lasheras *et al* [30], who alternatively proposed for bubbles in water:

$$f/f^* = c_1[\beta - 12(l^*/l)^{5/3}]^{1/2}, \tag{16}$$

where $\beta = 8.2$ was given by Batchelor [5]. Moreover, Chatzi and Lee [31] proposed for liquid–liquid dispersions that

$$f/f^* = c_1\Gamma[3/2, (l^*/l)^{5/3}]. \tag{17}$$

These models for turbulent breakage of dispersed phases (generally for liquid in gas, gas in liquid, and liquid–liquid) are plotted in figure 1 for illustration. Other authors (Narismhan *et al* [32], Luo and Svendsen [33], among many others) have proposed models for liquid–liquid dispersions with frequencies that do not decay, or tend to a constant, for l larger than l^*. For liquid droplets in gas, taking a broad approach to all the above models one may assume, as a first-order approximation, a flat dependence of the breakup-coalescence frequency for length scales around l^* and larger. Formally speaking, this means that $d(x, t)$ is assumed *flat* as a first approximation around $l \sim l^*$, which allows one to take, without loss of generality, $\Delta t \sim 1/f^*$.

In summary, one can choose Δt (time scaling) such that the product $d(x, t)\Delta t$ is of order unity along the process; this amounts to scale the frequency $d(x, t)$, so that $d(x, t)\Delta t \simeq g(x, t) \sim O(1)$, consistently with the finite difference scheme. In this work we do not aspire to model turbulent breakage, but to provide a new consistent mathematical tool to reflect the actual complexity of pdfs coming from turbulent breakage-coalescence by a few parameters. Indeed, our approximation $g(x, t) \simeq 1$ in one of the steps taken in the mathematical reduction proposed is consistent with the published literature. Then, for such processes whose homogeneity along the entire turbulent cascade would justify

$g(x, t) \simeq$ const, one can choose const. $= 1$ without lost of generality. In this case, one would conclude

$$p(x, t + \Delta t) = \int_0^\infty p^*(x/y, t) p(y, t)\, \mathrm{d}y/y, \tag{18}$$

which corresponds to the convolution of the pdf p with p^*.

Physically, expression (18) would describe how the pdf p would happen to be modulated by a generalized breakup process with governing pdf p^* at each finite step of the global process from the liquid discharge. Naturally, this involves an artificial reduction to a discrete step sequence from a natural 'continuous' process with a governing time scale, though. This same line of reasoning would directly lead to expression (18) if one starts from the pdf resulting from a typical ligament breakup (see references [15, 17]), and applies a self-convolution of that pdf as many times as the number of steps N are required by the process (this number should be one of the few parameters which the experimental results are reduced to). In this way, kernel (12) would have a clear physical interpretation: the pdf from a typical ligament breakup mentioned.

2.3. Using Mellin convolution to obtain closed expressions for N discrete steps

Expression (18) for $p(x, \Delta t)$ is the Mellin convolution of the functions $p(x, t)$ and $p^*(x, t)$ (see appendix A). Reducing the continuous process to a finite N-step scheme (where the time t in each step i, denoted by t_i, is given by $t_i = i \times \Delta t$, $i = 1, \ldots, N$), we can express

$$p_N(x) = \int_0^\infty p_1(x/y) p_{N-1}(y)\, \mathrm{d}y/y = p_1 \star p_{N-1}, \tag{19}$$

where $p_i(x) = p(x, t_i)$. Note that we have set $p_1 \equiv p^*$ for convenience and consistency with the physical interpretation given in the previous section. Denoting by $P_i(s)$ the Mellin transform of $p_i(x)$, the exchange formula (A.3) provides

$$P_N(s) = P_1(s) P_{N-1}(s). \tag{20}$$

Interestingly, since we assume a symmetry in the initial steps of the process, such that the initial distribution can be expressed as the kernel itself, the symmetry (and the commutative property of the convolution) of expression (20) proves the equality

$$\begin{aligned} p_1 \star p_{N-1} &= \int_0^\infty p_1(x/y) p_{N-1}(y)\, \mathrm{d}y/y \\ &= \int_0^\infty p_1(y) p_{N-1}(x/y)\, \mathrm{d}y/y = p_{N-1} \star p_1. \end{aligned} \tag{21}$$

Moreover, one could write for any step N

$$p_N(x) = \int_0^\infty p_i(x/y) p_j(y)\, \mathrm{d}y/y = p_i \star p_j, \qquad \forall\, (i, j)/N = i + j, \tag{22}$$

and inductively one obtains

$$p_N = \underbrace{p_1 \star p_1 \star \ldots \star p_1}_{N\text{times}}. \tag{23}$$

In summary, we propose that the discrete temporal scheme discussed can be faithfully reflected by the general transformation

$$\Upsilon[p(x), n] = p_n(x), \tag{24}$$

where n is any positive real number such that, when $n \in \mathbb{N}$, then $p_n = \underbrace{p \star \ldots \star p}_{n\text{times}}$.

As we will see in detail in the following sections, the properties of the Mellin transform shown in appendix A guarantee that our proposed transformation (24) leaves the structure present in (1) invariant, i.e.

$$p_N(x) = x^{\alpha-1} f_N(x), \tag{25}$$

and, therefore, we can express

$$\Upsilon[f(x), n] = f_n(x) \Longrightarrow p_n(x) = x^{\alpha-1}\Upsilon[f(x), n]. \tag{26}$$

3. Some practical applications

Once our general approach has been laid out in terms of a mathematical structure of a pdf as (1), consisting on (i) a potential pre-function which reflects into a single parameter the intensity of fragmentation events, and (ii) a function reflecting the discrete convolution steps of a basic pdf, we aim to apply these principles to two classical distributions. Some remarkable properties of the proposed transformation $\Upsilon[f(x), n]$ are then studied, arriving to some general conclusions supporting that real droplet/bubble size distributions could be faithfully projected on a relatively simple functional space whose metrics are provided by a small number of parameters with full physical meaning.

3.1. The log-normal distribution

We start our investigation applying our transformation (25) on a process where $p_1(x)$ and $p_n(x)$ can be expressed as log-normal distributions [34]. If our transformation (25) is consistent with the central limit theorem (CLT), it should leave invariant the log-normal structure and reduce the degree of convolution to a single parameter.

A log-normal distribution depends on two parameters μ and σ^2 and its probability density function is classically written as

$$p(x) = \frac{1}{x\sigma\sqrt{2\pi}}\, \mathrm{e}^{-\frac{(\ln x-\mu)^2}{2\sigma^2}}. \tag{27}$$

A fact about the log-normal distribution is that its median value is

$$x_{50} = \mathrm{e}^{\mu}. \tag{28}$$

We compute the Mellin transform of (27) as follows:

$$\begin{aligned} P(s) &= \frac{1}{\sigma\sqrt{2\pi}} \int_0^\infty x^{s-1} \frac{\mathrm{e}^{-\frac{(\ln x-\mu)^2}{2\sigma^2}}}{x}\, \mathrm{d}x \\ &= \frac{1}{\sigma\sqrt{2\pi}} \int_0^\infty \frac{\mathrm{e}^{-\frac{(\ln x-\mu)^2}{2\sigma^2}+(s-1)\ln x}}{x}\, \mathrm{d}x. \end{aligned} \tag{29}$$

Changing the variable of integration from x to $y = \frac{lnx}{\sigma}$:

$$P(s) = \frac{1}{\sqrt{2\pi}} \int_{-\infty}^\infty \mathrm{e}^{-\frac{(y-\mu/\sigma)^2}{2}+(s-1)y\sigma}\, \mathrm{d}y. \tag{30}$$

Now, completing the square in y, one has that

$$\begin{aligned} &-\frac{(y-\mu/\sigma)^2}{2} + (s-1)y\sigma \\ &\quad = -\frac{(y-(\mu/\sigma+(s-1)\sigma))^2}{2} + (s-1)\left(\mu + (s-1)\frac{\sigma^2}{2}\right). \end{aligned} \tag{31}$$

Hence,

$$P(s) = \frac{\mathrm{e}^{(s-1)(\mu+(s-1)\frac{\sigma^2}{2})}}{\sqrt{2\pi}} \int_{-\infty}^{\infty} \mathrm{e}^{-\frac{(y-(\mu/\sigma+(s-1)\sigma))^2}{2}} \mathrm{d}y, \tag{32}$$

and defining $z = \frac{y-(\mu/\sigma+(s-1)\sigma)}{\sqrt{2}}$:

$$P(s) = \frac{\mathrm{e}^{(s-1)(\mu+(s-1)\frac{\sigma^2}{2})}}{\sqrt{\pi}} \int_{-\infty}^{\infty} \mathrm{e}^{-z^2} \mathrm{d}z = \mathrm{e}^{(s-1)\left(\mu+(s-1)\frac{\sigma^2}{2}\right)}, \tag{33}$$

The normalization requirement that $\int_0^\infty xp(x)\,\mathrm{d}x = 1$ implies that $P(2) = 1$; hence,

$$P(2) = \mathrm{e}^{\mu+\frac{\sigma^2}{2}} = 1, \tag{34}$$

implying that $\sigma^2 = -2\mu$ and thus reducing the variety of log-normal distributions to a single parameter. Defining $\hat{\mu} = -\mu$ as such parameter, we obtain that

$$P(s) = \mathrm{e}^{\hat{\mu}(s-1)(s-2)}, \tag{35}$$

and the probability density function is reduced to

$$p(x) = \frac{1}{2x^{3/2}\sqrt{\pi\hat{\mu}}} \mathrm{e}^{-\frac{(\ln x)^2+\hat{\mu}^2}{4\hat{\mu}}}. \tag{36}$$

Written in the form $p(x) = x^{\alpha-1} f(x)$, one has $\alpha = -1/2$ and

$$f(x) = \frac{1}{2\sqrt{\pi\hat{\mu}}} \mathrm{e}^{-\frac{(\ln x)^2+\hat{\mu}^2}{4\hat{\mu}}}. \tag{37}$$

Taking p_1 to be a log-normal distribution of the above form, from (34), one obtains by continued use of the exchange formula the expression for the N-step distribution function of the process in Mellin space:

$$P_N(s) = P_1^N(s) = \mathrm{e}^{N\hat{\mu}(s-1)(s-2)}, \tag{38}$$

which implies that the distribution function is, for all N, again a log-normal distribution[1] with parameters $\mu_N = -N\hat{\mu}$ and $\sigma_N^2 = 2N\hat{\mu}$ and thus from the inversion formula

$$p_N(x) = \frac{1}{2x^{3/2}\sqrt{\pi N\hat{\mu}}} \mathrm{e}^{-\frac{(\ln x)^2+N^2\hat{\mu}^2}{4N\hat{\mu}}}, \tag{39}$$

from which

$$f_N(x) = \frac{1}{2\sqrt{\pi N\hat{\mu}}} \mathrm{e}^{-\frac{(\ln x)^2+(N\hat{\mu})^2}{4N\hat{\mu}}}. \tag{40}$$

This shows that the only relevant parameter which characterizes the distribution is $N\hat{\mu}$. In figure 2 we show the evolution of $p_N(x)$ as N increases for an example values of $\hat{\mu}$.

From this result and using (28), one obtains the count mean x_{50} as

$$x_{50} = \mathrm{e}^{-N\hat{\mu}}. \tag{41}$$

To study the mass median as defined by (5) we consider the probability distribution whose density function corresponds to $p'_N(x) = xp_N(x)$; the median of that probability distribution is the mass median.

Using the properties of the Mellin transform (see appendix A) we obtain that

$$P'_N(s) = P_N(s+1) = \mathrm{e}^{N\hat{\mu}s(s-1)} = \mathrm{e}^{(s-1)(N\hat{\mu}+N\hat{\mu}(s-1)}, \tag{42}$$

[1] This is a defining fact of the log-normal distribution: the product of log-normals is again log-normal.

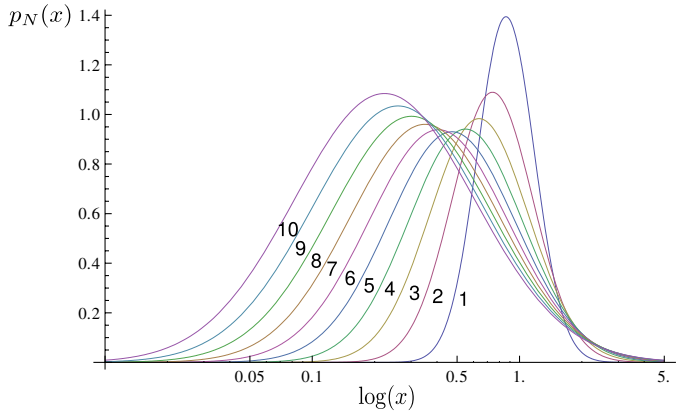

Figure 2. Plots of $p_N(x)$, for $N = 1, \ldots, 10$, when $p_1(x)$ is log-normal with $\hat{\mu} = 0.1$.

and comparing with (33) we see that $p'_N(x)$ is again the density function of a log-normal distribution with parameters $\mu'_N = N\hat{\mu}$ and $\sigma^2 = 2N\hat{\mu}$. Hence, its median (which is the mass median) is given by

$$y_{50} = \mathrm{e}^{N\hat{\mu}}, \tag{43}$$

from which we see that $x_{50} = y_{50}^{-1}$.

The cut-off mass size y_ϕ corresponding to a mass fraction ϕ for the N-step size distribution is obtained integrating $p'_N(x)$, which can be done explicitly using the complementary error function. The result is given by

$$\frac{1}{2}\mathrm{erfc}\left[\frac{N\mu - \ln y_\phi}{2\sqrt{\mu N}}\right] = \phi. \tag{44}$$

This expression, together with (43), provides a useful expression to relate y_ϕ and ϕ given y_{50} alone, i.e.

$$\mathrm{erfc}\left[\frac{\ln(y_{50}/y_\phi)}{2\sqrt{\ln y_{50}}}\right] = 2\phi. \tag{45}$$

The interesting thing about this result is that, if a certain single-step mass partition process can be represented by a log-normal distribution, then any subsequent N-step partition process can be represented by a log-normal distribution whose index N can be obtained from a single experimental measurement of y_{50}.

From an applied perspective, the answer to the important question of what would be the mass fraction ϕ put in sizes below a given y_ϕ for a process involving subsequent steps of simpler log-normal processes can be given from a single experimental determination of the *mass median* and the *mass mean* sizes, whose ratio is y_{50} (naturally, the non-dimensional mass median y_{50} is made non-dimensional with the *mass mean* size). And, more importantly, once y_{50} is determined, the index N is a direct measure of the degree of convolution of the global process. What makes the log-normal distribution and its N-convolution particularly interesting as a first approach toward a potentially systematic modeling of droplet size distributions is (i) its symmetric behavior for both small and large size populations, (ii) its physical correspondence with highly convoluted processes exhibiting a symmetry in both fragmentation and coalescence occurrence rates and (iii) the direct correspondence between the index N and the extension of subsequent fragmentation and coalescence processes. Thus, an experimental

fitting to a log-normal distribution may provide fundamental information on the physics of the atomization/mixing process itself, to investigate not only the classical fragmentation *cascade* but also its *coalescence cascade* counterpart. Incidentally, the convolution-index N is not restricted to natural numbers: for the particular case of the log-normal distribution, N can be generalizable to any real positive value. This is a natural generalization that overcomes the discrete nature of the finite-difference scheme (18) and provides additional support for the consistency of the proposed transformation (24).

3.2. The Fréchet distribution

Once the mathematical consistency of our proposed transformation with the CLT is shown, we aim to apply our procedure to explain the physical roots of rather general distributions used in the literature. The best-established closed analytical expressions for pdfs of sprays and emulsions have been classically introduced by experimental investigators concerned with the mathematical consistency of their proposals, aided by probability theory (e.g. [23–25]). In the case of the Fréchet distribution, its success is based on the accuracy by which experimentally measured distributions are fitted by the analytical model. In this section we provide a complete analysis of this pdf according to our procedures for its illustrative power. Now, we investigate the finite-step scheme applied to a process where $p_1(x)$ can be expressed as a Fréchet distribution [22]:

$$p(x) = ax^{\alpha-1}\,\mathrm{e}^{-bx^{\beta}}, \tag{46}$$

where a, b, α, β should be positive real numbers.

To obtain the Mellin transform $P(s)$ of $p(x)$, we use the properties listed in appendix A. Denoting $f(x) = \mathrm{e}^{-bx}$, we have that $P(s) = \frac{a}{\beta}F\left(\frac{s+\alpha-1}{\beta}\right)$, and since $F(s) = b^s\Gamma(s)$ (see appendix A), we obtain that

$$P(s) = \frac{a}{\beta}b^{\frac{s+\alpha-1}{\beta}}\Gamma\left(\frac{s+\alpha-1}{\beta}\right). \tag{47}$$

Again, the normalization requirements demand $P(1) = P(2) = 1$. Those requirements imply

$$\frac{a}{\beta}b^{\frac{\alpha}{\beta}}\Gamma\left(\frac{\alpha}{\beta}\right) = \frac{a}{\beta}b^{\frac{\alpha+1}{\beta}}\Gamma\left(\frac{\alpha+1}{\beta}\right) = 1. \tag{48}$$

Solving for a and b we obtain that

$$a = \beta\frac{\Gamma^{\alpha}\left(\frac{\alpha+1}{\beta}\right)}{\Gamma^{\alpha+1}\left(\frac{\alpha}{\beta}\right)}, \qquad b = \left[\frac{\Gamma\left(\frac{\alpha+1}{\beta}\right)}{\Gamma\left(\frac{\alpha}{\beta}\right)}\right]^{\beta}. \tag{49}$$

Thus, normalized Fréchet distributions are characterized by *two* parameters, namely α and β. The interest of these distributions is that the exponential ($\alpha = \beta = 1$), gamma ($\beta = 1$), and Rosin–Rammler distributions ($\alpha = \beta$), very common to model mass distributions in powders and sprays, are particular cases of the Fréchet ones. Inserting (49) in (47) we obtain the (normalized) Mellin transform of a Fréchet distribution:

$$P(s) = \frac{\Gamma\left(\frac{s+\alpha-1}{\beta}\right)\left[\Gamma\left(\frac{\alpha+1}{\beta}\right)\right]^{1-s}}{\left[\Gamma\left(\frac{\alpha}{\beta}\right)\right]^{2-s}}. \tag{50}$$

Obviously, for the exponential function, $P(s) = \Gamma(s)$.

The expression for the N-step distribution of the process is easy to obtain as a Mellin transform:

$$P_N(s) = \frac{\left[\Gamma\left(\frac{s+\alpha-1}{\beta}\right)\right]^{N}\left[\Gamma\left(\frac{\alpha+1}{\beta}\right)\right]^{N(1-s)}}{\left[\Gamma\left(\frac{\alpha}{\beta}\right)\right]^{N(2-s)}}. \tag{51}$$

To obtain the inverse Mellin transform, denote $F(s) = \left[\Gamma\left(\frac{s+\alpha-1}{\beta}\right)\right]^N$. Using the properties in appendix A, we obtain that

$$P_N(x) = \frac{\left[\Gamma\left(\frac{\alpha+1}{\beta}\right)\right]^N}{\left[\Gamma\left(\frac{\alpha}{\beta}\right)\right]^{2N}} f\left(\left[\frac{\Gamma\left(\frac{\alpha+1}{\beta}\right)}{\Gamma\left(\frac{\alpha}{\beta}\right)}\right]^N x\right). \tag{52}$$

It remains to obtain $f(x)$. For that we denote by $g(x)$ the inverse Mellin transform of $\Gamma^N(s)$ and note that, using again the properties listed in appendix A, we obtain

$$f(x) = \beta x^{(\alpha-1)} g(x^\beta), \tag{53}$$

so that using (52)

$$p_N(x) = \beta x^{(\alpha-1)} \frac{\left[\Gamma\left(\frac{\alpha+1}{\beta}\right)\right]^{N\alpha}}{\left[\Gamma\left(\frac{\alpha}{\beta}\right)\right]^{N(\alpha+1)}} g\left(\left[\frac{\Gamma\left(\frac{\alpha+1}{\beta}\right)}{\Gamma\left(\frac{\alpha}{\beta}\right)}\right]^{N\beta} x^\beta\right). \tag{54}$$

The function $g(x)$ is expressed, using the Mellin inverse transform of $\Gamma^N(s)$, as

$$g(x) = \frac{1}{2\pi \mathrm{i}} \int_{c-\mathrm{i}\infty}^{c+\mathrm{i}\infty} \Gamma^N(s) x^{-s}\, \mathrm{d}s, \tag{55}$$

where $c > 0$. Equation (55) is a Mellin–Barnes-type integral which can be expressed using the Meijer G function, also known as the generalized hypergeometric function, which is a special function of a very general type that allows us to express, among others, the hypergeometric, Bessel, trigonometric and exponential functions [35]. Writing (55) in terms of the Meijer G, we obtain

$$f(x) = G_{0,N}^{N,0}\left[x \,\middle|\, \begin{matrix} - \\ 0, \ldots, 0 \end{matrix}\right], \tag{56}$$

and using (54), we obtain

$$p_N(x) = \frac{\beta x^{\alpha-1}}{\left[\Gamma\left(\frac{\alpha}{\beta}\right)\right]^N} \left[\frac{\Gamma\left(\frac{\alpha+1}{\beta}\right)}{\Gamma\left(\frac{\alpha}{\beta}\right)}\right]^{N\alpha} G_{0,N}^{N,0}\left[\left[\frac{\Gamma\left(\frac{\alpha+1}{\beta}\right)}{\Gamma\left(\frac{\alpha}{\beta}\right)}\right]^{N\beta} x^\beta \,\middle|\, \begin{matrix} - \\ 0, \ldots, 0 \end{matrix}\right]. \tag{57}$$

Calling

$$c_1 = \frac{1}{\Gamma\left(\frac{\alpha}{\beta}\right)}, \qquad c_2 = \frac{\Gamma\left(\frac{\alpha+1}{\beta}\right)}{\Gamma\left(\frac{\alpha}{\beta}\right)}, \tag{58}$$

equation (57) is compactly expressed as

$$p_N(x) = \beta c_1^N c_2^{N\alpha} x^{\alpha-1} G_{0,N}^{N,0}\left[c_2^{N\beta} x^\beta \,\middle|\, \begin{matrix} - \\ 0, \ldots, 0 \end{matrix}\right], \tag{59}$$

which, using the properties of the Meijer G function can be further simplified to

$$p_N(x) = \beta c_1^N c_2^N G_{0,N}^{N,0}\left[c_2^{N\beta} x^\beta \,\middle|\, \begin{matrix} - \\ \frac{\alpha-1}{\beta}, \ldots, \frac{\alpha-1}{\beta} \end{matrix}\right]. \tag{60}$$

In figure 3 we show the evolution of $p_N(x)$ as N increases for example values of α and β. Note that the function $G_{0,N}^{N,0}$ in (60) has been already studied and written explicitly as a function of x and N in [36]. However, such expression is too involved to be useful in our context.

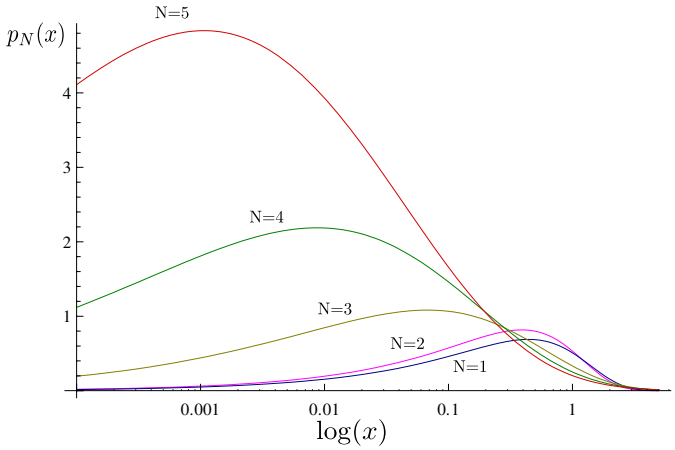

Figure 3. Plots of $p_N(x)$, for $N = 1, \ldots, 5$, when $p_1(x)$ is Fréchet with $\alpha = 1.5$, $\beta = 0.5$.

The most interesting property from an applied point of view is the mass median of the distribution function defined by (60). To obtain that function, one could in principle apply its definition (5) and note that

$$\begin{aligned}\int_0^{y_{50}} x p_N(x) &= \beta c_1^N c_2^N \int_0^{y_{50}} x G_{0,N}^{N,0}\left[c_2^{N\beta}x^\beta \,\middle|\, \begin{matrix} - \\ \frac{\alpha-1}{\beta}, \ldots, \frac{\alpha-1}{\beta}\end{matrix}\right] \mathrm{d}x \\ &= \beta c_1^N \int_0^{y_{50}} G_{0,N}^{N,0}\left[c_2^{N\beta}x^\beta \,\middle|\, \begin{matrix} - \\ \frac{\alpha}{\beta}, \ldots, \frac{\alpha}{\beta}\end{matrix}\right] \mathrm{d}x \\ &= \frac{c_1^N}{c_2^N}\left(\frac{c_2^N}{c_1^N} - G_{1,N+1}^{N+1,0}\left[c_2^{N\beta}y_{50}^\beta \,\middle|\, \begin{matrix} 1 \\ 0, \frac{\alpha+1}{\beta}, \ldots, \frac{\alpha+1}{\beta}\end{matrix}\right]\right), \end{aligned} \tag{61}$$

where we have used the fact that

$$\lim_{x\to 0} G_{1,N+1}^{N+1,0}\left[c_2^{N\beta}x^\beta \,\middle|\, \begin{matrix} 1 \\ 0, \frac{\alpha+1}{\beta}, \ldots, \frac{\alpha+1}{\beta}\end{matrix}\right] = \frac{c_2^N}{c_1^N}. \tag{62}$$

Hence the median can be computed numerically from the equation

$$G_{1,N+1}^{N+1,0}\left[c_2^{N\beta}y_{50}^\beta \,\middle|\, \begin{matrix} 1 \\ 0, \frac{\alpha+1}{\beta}, \ldots, \frac{\alpha+1}{\beta}\end{matrix}\right] = \frac{1}{2}\frac{c_2^N}{c_1^N}. \tag{63}$$

However, it would be desirable to obtain approximate analytical expressions for the median.

A first approach would be to note that $P_N(x)$ represents the product of N distribution functions. Hence using the CLT (see appendix B), we know that $p_N(x)$ tends to the distribution function of a log-normal.

Since we are interested in the mass median (5) we define $p'_N(x) = x p_N(x)$. Note that $P'_N(s) = P_N(s+1)$, that is

$$P'_N(s) = \frac{\left[\Gamma\left(\frac{s+\alpha}{\beta}\right)\right]^N \left[\Gamma\left(\frac{\alpha+1}{\beta}\right)\right]^{-Ns}}{\left[\Gamma\left(\frac{\alpha}{\beta}\right)\right]^{N(1-s)}}. \tag{64}$$

From the CLT, we know that as N grows to infinity, $P'_N(s) \to \mathrm{e}^{(s-1)(\mu+(s-1)\frac{\sigma^2}{2})}$, the Mellin transform of a log-normal density function, where

$$\mu = N\int_0^\infty \ln x p'_1(x)\,\mathrm{d}x = N\frac{\mathrm{d}}{\mathrm{d}s}P'_1(s)\bigg|_{s=1}, \tag{65}$$

$$\begin{aligned}\sigma^2 &= N\int_0^\infty (\ln x)^2 p'_1(x)\,\mathrm{d}x - \left(\int_0^\infty \ln x p'_1(x)\,\mathrm{d}x\right)^2 \\ &= N\left(\frac{\mathrm{d}^2}{\mathrm{d}s^2}P'_1(s) - \left(\frac{\mathrm{d}}{\mathrm{d}s}P'_1(s)\right)^2\right)_{s=1}.\end{aligned} \tag{66}$$

Computing μ and σ^2, we obtain that

$$\begin{aligned}\mu &= N\left(\frac{1}{\beta}\Psi^{(0)}\left(\frac{\alpha+1}{\beta}\right) - \ln\left(\frac{\Gamma\left(\frac{\alpha+1}{\beta}\right)}{\Gamma\left(\frac{\alpha}{\beta}\right)}\right)\right) \\ \sigma^2 &= N\frac{1}{\beta^2}\Psi^{(1)}\left(\frac{\alpha+1}{\beta}\right),\end{aligned} \tag{67}$$

where $\Psi^{(j)}$ is the poly-gamma function of order j [37]. Hence the mass median of $p_N(x)$ will tend asymptotically to the median of a log-normal distribution which will be given by

$$y_{50} \to \mathrm{e}^{\mu} = \left[\frac{\Gamma\left(\frac{\alpha}{\beta}\right)}{\Gamma\left(\frac{\alpha+1}{\beta}\right)}\right]^N \mathrm{e}^{\frac{N}{\beta}\Psi^{(0)}\left(\frac{\alpha+1}{\beta}\right)}. \tag{68}$$

However, the approximation given by (68) is only good for large N; it would be desirable to obtain an approximation containing terms of order less than $O(N)$, i.e. an asymptotic expansion in N.

To do this, we use the Cornish–Fisher (C–F) expansion (see appendix C) as follows. Call by X'_n the random variable whose probability density function is given by $p'_N(x)$. We use the C–F expansion to obtain the 0.50 quantile of $Y' = \ln X'_n$, which we denote by $\hat{q}$. Then $y_{50} = \mathrm{e}^{\hat{q}}$. The reason to use a logarithmic transformation is that $\ln X'_n$ will, by the CLT, resemble more closely a normal.

To compute the C–F expansion we need to obtain the cumulants of Y'. From the definition of the cumulant-generating function, which we denote by $g_Y(z)$, one has:

$$g_Y(z) = \ln E[\mathrm{e}^{zY'}] = \ln E\left[X'^z_n\right] = \ln\left(\int_0^\infty x^z p'_N(x)\,\mathrm{d}x\right) = \ln P'_N(z+1). \tag{69}$$

Then, the cumulants κ_j are defined as

$$\kappa_j = \frac{\mathrm{d}^j}{\mathrm{d}z^j}g_Y(z)|_{z=0} = \frac{\mathrm{d}^j}{\mathrm{d}s^j}(\ln P'_N(s))_{s=1}. \tag{70}$$

Using (64) we have that

$$\ln P'_N(s) = N\ln\Gamma\left(\frac{s+\alpha}{\beta}\right) - Ns\ln\left[\Gamma\left(\frac{\alpha+1}{\beta}\right)\right] - N(1-s)\ln\left[\Gamma\left(\frac{\alpha}{\beta}\right)\right], \tag{71}$$

and hence can obtain an expression for κ_j as follows:

$$\kappa_1 = N\left(\frac{1}{\beta}\Psi^0\left(\frac{\alpha+1}{\beta}\right) + \ln\left[\frac{\Gamma\left(\frac{\alpha}{\beta}\right)}{\Gamma\left(\frac{\alpha+1}{\beta}\right)}\right]\right), \tag{72}$$

$$\kappa_j = \frac{N}{\beta^j}\Psi^{(j-1)}\left(\frac{\alpha+1}{\beta}\right), \qquad j > 1. \tag{73}$$

Following the procedure in appendix C, we obtain that

$$\mu = \kappa_1 = N\left(\frac{1}{\beta}\Psi^0\left(\frac{\alpha+1}{\beta}\right) + \ln\left[\frac{\Gamma\left(\frac{\alpha}{\beta}\right)}{\Gamma\left(\frac{\alpha+1}{\beta}\right)}\right]\right), \tag{74}$$

$$\sigma^2 = \kappa_2 = \frac{N}{\beta^2}\Psi^{(1)}\left(\frac{\alpha+1}{\beta}\right), \tag{75}$$

$$\kappa_1^* = \kappa_2^* = 0,\ \kappa_j^* = \frac{\kappa_j}{\sigma^j} = N^{1-j/2}\frac{\Psi^{(j-1)}\left(\frac{\alpha+1}{\beta}\right)}{\left[\Psi^{(1)}\left(\frac{\alpha+1}{\beta}\right)\right]^{j/2}}, \qquad j \geqslant 3, \tag{76}$$

so defining $\hat{q}^* = \frac{\hat{q}-\mu}{\sigma}$, we obtain the C–F expansion for $\hat{q}^*$ as follows:

$$\hat{q}^* \approx -\tfrac{1}{6}\kappa_3^* + \tfrac{1}{40}\kappa_5^* - \tfrac{1}{12}\kappa_3^*\kappa_4^* + \tfrac{17}{324}(\kappa_3^*)^3, \tag{77}$$

where we have used that $\Phi_N^{-1}(0.50) = 0$. Solving for $\hat{q}$ as a function of the cumulants and using that $y_{50} = \mathrm{e}^{\hat{q}}$, we then obtain

$$y_{50} \approx \mathrm{e}^{\mu - \frac{\sigma}{6}\kappa_3^* + \frac{\sigma}{40}\kappa_5^* - \frac{\sigma}{12}\kappa_3^*\kappa_4^* + \frac{17\sigma}{324}(\kappa_3^*)^3}, \tag{78}$$

which can be written in terms of the parameters as

$$\begin{aligned} y_{50} \approx \left[\frac{\Gamma\left(\frac{\alpha}{\beta}\right)}{\Gamma\left(\frac{\alpha+1}{\beta}\right)}\right]^N \exp\Bigg\{ & \frac{N}{\beta}\Psi^{(0)}\left(\frac{\alpha+1}{\beta}\right) - \frac{1}{6\beta}\frac{\Psi^{(2)}\left(\frac{\alpha+1}{\beta}\right)}{\Psi^{(1)}\left(\frac{\alpha+1}{\beta}\right)} \\ & + \frac{N^{-1}}{40\beta}\frac{\Psi^{(4)}\left(\frac{\alpha+1}{\beta}\right)}{\left[\Psi^{(1)}\left(\frac{\alpha+1}{\beta}\right)\right]^2} - N^{-1}\frac{\Psi^{(2)}\left(\frac{\alpha+1}{\beta}\right)}{324\beta\left[\Psi^{(1)}\left(\frac{\alpha+1}{\beta}\right)\right]^4} \\ & \times\left[27\Psi^{(1)}\left(\frac{\alpha+1}{\beta}\right)\Psi^{(3)}\left(\frac{\alpha+1}{\beta}\right) - 17\left[\Psi^{(2)}\left(\frac{\alpha+1}{\beta}\right)\right]^2\right]\Bigg\}. \end{aligned} \tag{79}$$

Discarding the terms of order N^{-1}, we obtain a good enough approximation for most cases:

$$y_{50} \approx \left[\frac{\Gamma\left(\frac{\alpha}{\beta}\right)}{\Gamma\left(\frac{\alpha+1}{\beta}\right)}\right]^N \exp\left\{\frac{N}{\beta}\Psi^{(0)}\left(\frac{\alpha+1}{\beta}\right) - \frac{1}{6\beta}\frac{\Psi^{(2)}\left(\frac{\alpha+1}{\beta}\right)}{\Psi^{(1)}\left(\frac{\alpha+1}{\beta}\right)}\right\}. \tag{80}$$

Note that the C–F expansion can be used not only for the mass median, but for any other mass fraction, by following the procedure outlined in appendix C. Also, if necessary, more terms could be added to the expansion.

Like in the case of the log-normal distribution, the above expression allows the calculation of the index N from a measurement where y_{50} is determined, assuming a known process where a single-step mass partition can be modeled by a Fréchet distribution with α and β known beforehand. In fact, from expression (80), one can explicitly express N as a function of y_{50}:

$$N = \frac{\ln(y_{50}) + \frac{1}{6\beta}\frac{\Psi^{(2)}\left(\frac{\alpha+1}{\beta}\right)}{\Psi^{(1)}\left(\frac{\alpha+1}{\beta}\right)}}{\ln\left\{\frac{\Gamma\left(\frac{\alpha}{\beta}\right)}{\Gamma\left(\frac{\alpha+1}{\beta}\right)}\right\} + \frac{1}{\beta}\Psi^{(0)}\left(\frac{\alpha+1}{\beta}\right)}. \tag{81}$$

Thus, using the above approximate expression for N given y_{50}, one can calculate the mass fraction given y_ϕ using the C–F expansion.

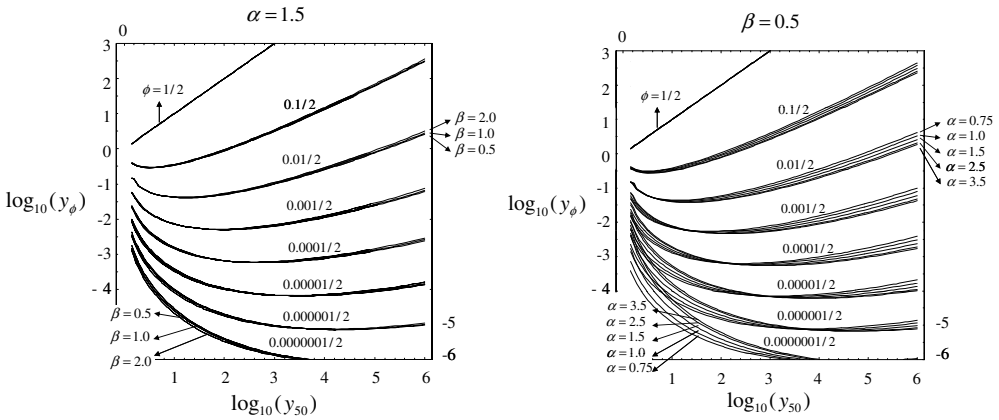

Figure 4. The mass fraction ϕ as a function of y_{50} and y_ϕ for several values of α and β: (a) fixed $\alpha = 1.5$, and (b) fixed $\beta = 0.5$.

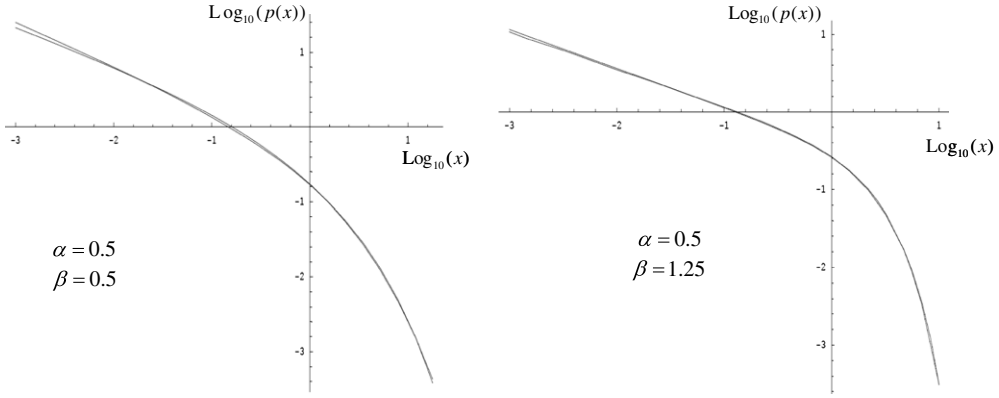

Figure 5. Combined plots of pdfs for both Féchet and transformed gamma ($\beta = 1$, and N given by expression (82)) sharing the same mass median y_{50}, for example values of α and β. Note the very small discrepancy found over the physical domain where the functions should work.

Again, it is important to emphasize that, from the practical view, N is an intermediate factor with a high physical meaning proportional to $\ln(y_{50})$. Note that this is the same dependence for the log-normal distribution as well (see (43)). From that meaning of N, the magnitude of y_{50} indicates the 'degree of convolution' of a process: the larger y_{50}, the wider the size distribution is, indicating a process undergoing a large number N of partition steps. Figure 4 provides the values of the mass fraction ϕ as a function of y_{50} and y_ϕ for several values of α and β.

From the applied, practical view, a series of interesting results arise from the analysis just outlined. For example, the Fréchet distribution can be very accurately approximated by the function resulting from the transformation $\Upsilon[p(x), N]$ applied on a gamma distribution searching for the appropriate value of N, and this value can be easily obtained using approximation (81). In effect, the gamma distribution corresponds to a Fréchet with $\beta = 1$. Then, equating the value of the mass median y_{50} of a transformed gamma with parameter N

(equation (80) with parameter $\beta = 1$), and that of a Fréchet (equation (80) with parameter $N = 1$), one easily obtains

$$N = \frac{\ln\left\{\frac{\Gamma\left(\frac{\alpha}{\beta}\right)}{\Gamma\left(\frac{\alpha+1}{\beta}\right)}\right\} + \frac{1}{\beta}\Psi^{(0)}\left(\frac{\alpha+1}{\beta}\right) - \frac{1}{6\beta}\frac{\Psi^{(2)}\left(\frac{\alpha+1}{\beta}\right)}{\Psi^{(1)}\left(\frac{\alpha+1}{\beta}\right)}}{-\ln\alpha + \Psi^{(0)}(\alpha+1) - \frac{1}{6}\frac{\Psi^{(2)}(\alpha+1)}{\Psi^{(1)}(\alpha+1)}}. \tag{82}$$

This result is supported by the very interesting fact that for a given value of α, the differences among transformed Fréchet distributions with different β values but sharing the same median size y_{50} are negligible, for an ample range of β values (see figure 5).

Therefore, equation (82) would constitute a closed, approximate but useful expression for the 'degree of convolution' N of a gamma distribution due to ligament breakup mechanisms [15–17] in a real spray whose experimental pdf is fitted by a Fréchet distribution with parameters α and β. Moreover, like in the case of the log-normal distribution, N is not restricted to natural numbers, consistently with the continuous nature of the parameter β. These results justify the success of this particular pdf to describe the droplet size distribution in sprays.

4. Conclusions

In this work, we propose a consistent operational calculus framework derived from dynamical arguments to characterize droplet/bubble size distributions resulting from turbulent breakup of an immiscible fluid into a carrier one. Starting from a finite-difference formulation of the integro-differential continuous coagulation and fragmentation equation, we show that the dynamical processes taking place in a random breakup/coalescence process of a disperse phase may exhibit the same structure as a discrete sequence of Mellin convolutions between the probability distribution of the evolving disperse phase and a generic kernel. This kernel may have its physical correspondence with the probability distribution resulting from a single breakup event, e.g. a liquid ligament breakup in a ligament-mediated spray formation [15, 16]. A natural consequence of the dynamical reduction proposed is that the number of convolution steps in the sequence can be reduced to a single parameter. To illustrate the physical faithfulness of our proposed parametrical reduction, we apply our procedure to the exponential and the gamma distributions to obtain the Fréchet distribution (earlier used by Rosin and Rammler (23), and by Nukiyama and Tanasawa (24)). This provides a physical foundation for the success of this particular probability density function in accurately fitting experimentally measured droplet size distributions in sprays and emulsions, and opens a new avenue for the exploration and generalization of other novel model distributions, e.g. one that have recently shown an apparently strong fitting power [38].

Appendix A. Mellin transform: definition and selected properties

Perhaps less known than other integral transforms, the Mellin transform [39] is an useful tool that can be used to simplify problems involving *products* of probability distributions, in a similar way that the Laplace transform is used in situations involving sums of probability distributions.

Given a function $f(x)$ defined for nonnegative values of x, its Mellin transform $F(s)$ is defined as

$$F(s) = \int_0^\infty f(x)x^{s-1}\,\mathrm{d}x, \tag{A.1}$$

where s is a complex-valued variable, $s = \sigma + \mathrm{i}\omega$. In general integral (A.1) will only exist for some values of s such that $a_1 < a < a_2$, known as its *strip of definition*.

For example, if $f(x) = \mathrm{e}^{-px}$, $p > 0$, then $F(s) = p^{-s}\Gamma(s)$, where $\Gamma(s)$ is the Euler gamma function; this can be seen directly from (A.1) inserting $f(x) = \mathrm{e}^{-px}$ and changing the variable of integration from x to px.

From $F(s)$ one can recover the original $f(x)$ using the inverse Mellin transform, which is defined as follows:

$$f(x) = \frac{1}{2\pi\mathrm{i}} \int_{a-i\infty}^{a+i\infty} F(s)x^{-s}\,\mathrm{d}s, \tag{A.2}$$

where the integration in (A.2) is done in the complex plane along the line $\mathrm{Re}(s) = a$ (which must lie inside the strip of definition). This integral is in general hard to evaluate, but can sometimes be computed using the method of residues.

From the point of view of probability theory, the most interesting property of the Mellin transform is the exchange formula relating the transform of two functions and their multiplicative convolution. Given two functions $f(x)$ and $g(x)$ their multiplicative convolution $h(x)$, which we write as $h(x) = f(x) \star g(x)$, is defined as

$$h(x) = \int_0^\infty f(y)g\left(\frac{x}{y}\right)\frac{\mathrm{d}y}{y}. \tag{A.3}$$

The Mellin exchange formula gives the Mellin transform of the convolution as $H(s) = F(s)G(s)$. Note that this implies the commutativity of the convolution, i.e. $f(x) \star g(x) = g(x) \star f(x)$.

The interest of multiplicative convolution for probability theory is the following. If $f(x)$ and $g(x)$ are the *probability density functions* of two (positive) random variables X_1 and X_2, then the density function of the random variable X_3 defined as the *product* of X_1 and X_2, i.e. $X_3 = X_1X_2$, is given by the multiplicative convolution as defined in (A.3). Thus, the Mellin transform can be used as a tool to obtain, using the exchange formula, the probability density function of products of two or more random variables.

Next we summarize other useful properties of the Mellin transform, in which we assume that $F(s)$ is the Mellin transform of a function $f(x)$.

(i) The Mellin transform of $f(px)$, for $p > 0$, is given by $p^{-s}F(s)$.
(ii) The Mellin transform of $f(x^a)$, $a > 0$, is given by $\frac{1}{a}F\left(\frac{s}{a}\right)$.
(iii) The Melllin transform of $x^z f(x)$ is $F(s + z)$.
(iv) The Mellin transform of $(\ln x)^n f(x)$, n a positive integer, is $\frac{\mathrm{d}^n}{\mathrm{d}s^n}F(s)$.

Appendix B. The central limit theorem for products of positive random variables

The central limit theorem (CLT) is a well-known fact in probability theory. Given n independent, identically distributed (i.i.d.) random variables denoted by X_i, $i = 1, \ldots, n$, with mean μ and variance σ^2 then, under very mild conditions, when $n \to \infty$, one has that

$$\frac{\sum_{i=1}^n X_i - n\mu}{\sigma\sqrt{n}} \to N(0, 1), \tag{B.1}$$

where $N(m, s^2)$ denotes the normal distribution with mean m and variance s^2. This is convergence in distribution. Using the properties of the normal, we can write that

$$\sum_{i=1}^n X_i \to N(n\mu, n\sigma^2), \tag{B.2}$$

taking into account that the right-hand side of (B.2) diverges as n goes to infinity, so it has to be interpreted as an asymptotic expansion.

To handle a product of *positive* i.i.d. random variables [40], we take into account that

$$\prod_{i=1}^{n} X_i = \exp\left(\ln \prod_{i=1}^{n} X_i\right) = \exp\left(\sum_{i=1}^{n} \ln X_i\right), \tag{B.3}$$

and defining $Y_i = \ln X_i$, we obtain that

$$\prod_{i=1}^{n} X_i = \exp\left(\sum_{i=1}^{n} Y_i\right) \to \exp\left(N\left(n\mu_Y, n\sigma_Y^2\right)\right) = \mathrm{LogN}\left(n\mu_Y, n\sigma_Y^2\right), \tag{B.4}$$

which is the CLT for products of random variables. In (B.4), $\mathrm{logN}(m, s^2)$ is the log-normal distribution with parameters m and s^2, and μ_Y and σ_Y^2 are respectively the mean and variance of the variables Y_i, which are computed from the density function $f(x)$ of the variables X_i as follows:

$$\mu_Y = E[Y_i] = E[\ln X_i] = \int_0^\infty \ln x f(x)\,\mathrm{d}x, \tag{B.5}$$

$$\sigma_Y^2 = E\left[Y_i^2\right] - E[Y_i]^2 = E[(\ln X)^2] - \mu_Y^2 = \int_0^\infty (\ln x)^2 f(x)\,\mathrm{d}x - \mu_Y^2. \tag{B.6}$$

Appendix C. Cumulants and the Cornish–Fisher expansion

When characterizing droplet size populations with probability distributions, it is important to know not only density functions (or moments), but also quantiles such as the median and mass median. Cornish and Fisher developed an expansion for approximating the q-quantiles of a random variable X using only its first few cumulants [41].

Cumulants of a random variable X are formally defined using the cumulant-generating function $g(t)$ defined as

$$g(z) = \ln(E[\mathrm{e}^{zX}]), \tag{C.1}$$

i.e. as the logarithm of the moment-generating function. The nth cumulant κ_n is then defined as the nth derivative of $g(z)$ at $z = 0$:

$$\kappa_n = g^{(n)}(0). \tag{C.2}$$

Note that $\kappa_1 = \mu$ and $\kappa_2 = \sigma^2$, respectively the mean and variance of X. To compute the next cumulants of X up to order 5 we can use the following formulas:

$$\kappa_3 = \mu_3',\ \kappa_4 = \mu_4' - 3(\mu_2')^2,\ \kappa_5 = \mu_5' - 10\mu_3'\mu_2', \tag{C.3}$$

where μ_j' are the central moments of order j defined as

$$\mu_j' = E[(X - \mu)^j]. \tag{C.4}$$

Next we show the Cornish–Fisher asymptotic expansion. Assume first that X has zero mean and standard deviation 1. Then the q-quantile of X, $\Phi_X^{-1}(q)$, can be approximated using the first five cumulants of X as

$$\begin{aligned}\Phi_X^{-1}(q) \approx \Phi_N^{-1}(q) &+ \frac{\Phi_N^{-1}(q)^2 - 1}{6}\kappa_3 + \frac{\Phi_N^{-1}(q)^3 - 3\Phi_N^{-1}(q)}{24}\kappa_4 \\ &- \frac{2\Phi_N^{-1}(q)^3 - 5\Phi_N^{-1}(q)}{36}\kappa_3^2 + \frac{\Phi_N^{-1}(q)^4 - 6\Phi_N^{-1}(q)^2 + 3}{120}\kappa_5 \\ &- \frac{\Phi_N^{-1}(q)^4 - 5\Phi_N^{-1}(q)^2 + 2}{24}\kappa_3\kappa_4 + \frac{12\Phi_N^{-1}(q)^4 - 53\Phi_N^{-1}(q)^2 + 17}{324}\kappa_3^3,\end{aligned} \tag{C.5}$$

where $\Phi_N^{-1}(q)$ is the q-quantile of a standard normal random variable $N(0, 1)$. If X has mean μ and standard deviation σ, define the normalization of X, denoted as X^*, as

$$X^* = \frac{X - \mu}{\sigma}, \tag{C.6}$$

and use the Cornish–Fisher expansion (C.5) to obtain $\Phi_{X^*}^{-1}(q)$. Note that the central moments $\mu_j'^*$ of X^* are obtained from the central moments of X as

$$\mu_1'^* = 0, \quad \mu_2'^* = 1, \qquad \mu_j'^* = \frac{\mu_j'}{\sigma^j}, \qquad j \geqslant 3, \tag{C.7}$$

and similarly the cumulants are given by

$$\kappa_1^* = 0, \quad \kappa_2^* = 1, \qquad \kappa_j^* = \frac{\kappa_j}{\sigma^j}, \qquad j \geqslant 3, \tag{C.8}$$

Then the q-quantile of X is recovered as

$$\Phi_X^{-1}(q) = \sigma \Phi_{X^*}^{-1}(q) + \mu. \tag{C.9}$$

References

[1] Turner M S 2009 A century of physics: 1950 to 2050 *Phys. Today* **62** 8–9
[2] Kolmogorov A N 1949 On the breakage of drops in a turbulent flow *Dokl. Akad. Navk. SSSR* **66** 825–8
[3] Hinze J O 1955 Fundamentals of the hydrodynamics mechanisms of splitting in dispersion process *AIChE J.* **1** 289–95
[4] Lasheras J C, Eastwood C, Martínez-Bazán C and Montañes J L 2002 A review of statistical models for the break-up of an immiscible fluid immersed into a fully developed turbulent flow *Int. J. Multiph. Flow* **28** 247–78
[5] Batchelor G K 1953 *The Theory of Homogeneous Turbulence* (Cambridge: Cambridge University Press)
[6] Friedlander S K and Wang C S 1967 The self-preserving particle size distribution for coagulation by Brownian motion *J. Colloid Interface Sci.* **22** 126–32
[7] Wang C S and Friedlander S K 1967 The self-preserving particle size distribution for coagulation by Brownian motion II: small particle slip correction and simultaneous shear flow *J. Colloid Interface Sci.* **24** 170–9
[8] Mulholland G W, Lee T G and Baum H R 1977 The coagulation of aerosols with broad initial size distributions *J. Colloid Interface Sci.* **62** 406–20
[9] Baumann G, Freyberger M, Glockle W G and Nonnenmacher T F 1991 Similarity solutions in fragmentation kinetics *J. Phys. A: Math. Gen.* **24** 5085–96
[10] Lamb W 2004 Existence and uniqueness results for the continuous coagulation and fragmentation equation *Math. Methods Appl. Sci.* **27** 703–21
[11] Cohen R D 1991 Shattering of a liquid drop due to impact *Proc. R. Soc.* A **435** 483–503
[12] Longuet-Higgins M S 1992 The crushing of air cavities in a liquid *Proc. R. Soc.* A **439** 611–26
[13] Novikov E A 1994 Infinitely divisible distributions in turbulence *Phys. Rev.* E **50** R3303–5
[14] Novikov E A and Dommermuth D G 1997 Distribution of droplets in a turbulent spray *Phys. Rev.* E **56** 5479–82
[15] Villermaux E, Marmottant Ph and Duplat J 2004 Ligament-mediated spray formation *Phys. Rev. Lett.* **92** 074501
[16] Marmottant Ph and Villermaux E 2004 Ligament-mediated spray formation *J. Fluid Mech.* **498** 73–111
[17] Eggers J and Villermaux E 2008 Physics of liquid jets *Rep. Prog. Phys.* **71** 036601
[18] Villermaux E and Bosa B 2009 Single-drop fragmentation determines size distribution of raindrops *Nature Phys.* **5** 697–702
[19] Cheng Z and Redner S 1990 Kinetics of fragmentation *J. Phys. A: Math. Gen.* **23** 1233–58
[20] Treat R P 1997 On the similarity solution of the fragmentation equation *J. Phys. A: Math. Gen.* **30** 2519–43
[21] McGrady E D and Ziff R M 1997 'Shattering' transition in fragmentation *Phys. Rev. Lett.* **58** 892–5
[22] Fréchet M 1927 Sur la loi de probabilité de l'écart maximum *Ann. Société Polonaise de Mathematique, Crocovie* **6** 93–116
[23] Rosin P and Rammler E 1934 Die kornzusammensetzung des mahlgutes im lichte der wahrscheinlichkeitslehre *Kolloid-Zeitschrift* **67** 16–26
[24] Nukiyama S and Tanasawa Y 1939 Experiments on the atomization of liquids in an air stream *Trans. Soc. Mech. Eng. Japan* **5** 62–7
[25] Weibull W 1951 A statistical distribution function of wide applicability *Trans. ASME, J. Appl. Mech.* **18** 293–7

[26] Cañizo J A 2007 Convergence to equilibrium for the discrete coagulation-fragmentation equations with detailed balance *J Stat. Phys.* **129** 1–26
[27] Ernst M H and Szamel G 1993 Fragmentation kinetics *J. Phys. A: Math. Gen.* **26** 6085–91
[28] Ross S L and Curl R L 1973 Measurements and models of the dispersed phase mixing process *Joint Chemical Engineering Conf. (Vancouver)* Paper 29b
[29] Coulaloglou C A and Tavlarides L L 1977 Description of interaction processes in agitated liquid–liquid dispersions *Chem. Eng. Sci.* **32** 1289
[30] Lasheras J C, Eastwood C, Martínez-Bazán C and Montañés J L 2002 A review of statistical models for the break-up of an immiscible fluid immersed into a fully developed turbulent flow *Int. J. Multiph. Flow* **28** 247–78
[31] Chatzi E and Lee J M 1987 Analysis of interactions for liquid–liquid dispersions in agitated vessels *Ind. Eng. Chem. Res.* **26** 2263
[32] Narismhan G, Gupta J P and Ramkrishna D 1979 A model for transitional breakage probability of droplets in agitated lean liquid–liquid dispersions *Chem. Eng. Sci.* **34** 257–65
[33] Luo H and Svendsen H F 1996 Theoretical model for drop and bubble breakup in turbulent dispersions *AIChE J.* **42** 1225–33
[34] Finney D J 1941 On the distribution of a variate whose logarithm is normally distributed *J. R. Stat. Soc.* **7** (suppl.) 155–61
[35] Mathai A M and Saxena R K 1973 *Generalized Hypergeometric Functions with Applications in Statistics and Physical Sciences* (Berlin: Springer)
[36] Springer M D and Thompson W E 1970 The distribution of products of beta, gamma and Gaussian random variables *SIAM J. Appl. Math.* **18** 721–37
[37] Erdelyi A, Magnus W, Oberhettinger F and Tricomi F G 1953 *Higher Transcendental Functions* vol 2 (New York: McGraw-Hill)
[38] Alexandrov M D and Lacis A A 2000 A new three-parameter cloud/aerosol particle size distribution based on the generalized inverse Gaussian density function *Appl. Math. Comput.* **116** 153–65
[39] Oberhettinger F 1974 *Tables of Mellin Transforms* (Berlin: Springer)
[40] Broadbent S R 1956 Lognormal approximation to products and quotients *Biometrika* **43** 404–17
[41] Kendall M G 1945 *The Advanced Theory of Statistics* (London: Charles Griffin)